Engineering and Technology Journal
Journal homepage: engtechjournal.org

Effect of Adding Silver Element and Zirconia Ceramic on Corrosion Behavior and Mechanical Properties of Pure Titanium

Wehad A. Al-Rawy [a*], **Emad S. Al-Hassani** [b]

[a] Materials Engineering Department- University of Technology, Baghdad, Iraq, wehadayad@gmail.com

[b] Materials Engineering Department- University of Technology, Baghdad, Iraq, 130042@uotechnology.edu.iq

* Corresponding author.

Submitted: 30/10/2019 Accepted: 22/12/2019 Published: 25/05/2021

K E Y W O R D S

Implant material, Dentistry, Titanium, Titanium alloys, Biocompatibility, Corrosion.

A B S T R A C T

In this research, all the samples are prepared using the powder metallurgy technique by adding silver element and Zirconia ceramic material to the commercially pure titanium at a different weight percent of (10, 20 and 30) to investigate the effect of adding these materials to the CP-Ti on corrosion behavior and mechanical properties. There are two sets of each type of alloys Ti-Ag and Ti ZrO_2. The Preparation process was by Weighing, Mixing and Homogenizing Powders by Ball Mill, compacting at 4 tons for 1 min. and Sintering at 700 and 900 ℃ for 2 hrs. under a controlled atmosphere. The corrosion results showed a good corrosion resistance increases with increasing the silver content as the corrosion rate would be the best in (30% Ag) content with(0.091 mpy) at sintering temperature of 700 ℃. And with a sintering temperature of 900 ℃, the best result was with (30% Ag) with (0.059) mpy. In the Ti-ZrO_2 alloys, the best result was with the zirconia content of (30%ZrO_2) when cooled in the air with (1.347) mpy at sintering temperature of 700 ℃, this results obtained in Ringer's solution. And microstructures analysis stated that at the silver and the Zirconia content of (10-20 wt%) single phase of (α- Ti alloy), as the silver and Zirconia content increased to (30% wt), in addition to (α-phase), (Ti2Ag) intermetallic compound developed in the silver alloy microstructure and (TiZr)3O intermetallic compound developed in the microstructure of Ti- Zirconia composites and the hardness test result best hardness of titanium-silver alloys is with a silver content of (30% Wt) at sintering temperature of 900 ℃.

How to cite this article: W.A. Al-Rawy, E.S. Al-Hassani, "Effect of adding silver element and zirconia ceramic on corrosion behavior and mechanical properties of pure titanium ," Engineering and Technology Journal Vol. 39, No. 05, pp. 674-694, 2021.
DOI: https://doi.org/10.30684/etj.v39i5A.1087

1. INTRODUCTION

Bimetallic elements are utilized for manufactured joints, manufactured bones, bone illustrations and pins, orthodontic lines, dental inserts, and maxillofacial illustrations and pins [1]. Besides the improvement of medical advances, with an expanded interest in materials by modern properties. Even though Ti and its compounds in organic forms possess astounding erosion obstruction, biocompatibility, also low specific gravity, all possess hindrances of low quality, low wear opposition, hydrogen embrittlement, is also troubling in assembling, welding, and machining [2-3]. Consequently, new elements clear from the disservices concerning Ti plus its combinations are needed. The explanations behind utilizing Ti and its composites as biomaterials incorporate their phenomenal consumption obstruction, absence of poisonous quality, absence of unfavorably susceptible response in touch among cell tissue, plus low flexible modulus [3-5]. As far as organic responses, most utmost metallic elements come into the biotolerant element class, however, Ti is some of the time arranged as a bioinert element [6]. This implies the surface of Ti has positive qualities as far as its response to natural tissues. There were opinions that the surface oxide of Ti is latent when in touch with organic tissue and that the development of collagen in the outside of titanium parts advances the development of new bone tissue [7]. Ti-Ag alloy possesses higher mechanical properties and erosion opposition than Ti and toxicities that were like Ti. Subsequently, it is suggested that titanium–silver composites be embraced mindfully by the biomedical and dental field [8].

This research also studies ZrO_2-Ti composites which including ZrO_2/Ti functionally graded materials (FGMs), which are appealing in entirely unexpected fields of both biomedical and aerospace industries. In view of biocompatibility of Ti because of its non-poisonous quality and non-dismissal of the human body, Ti has been extensively in medical fields, which can be utilized for surgical implements and implants. ZrO_2 - scattered Ti matrix composites have been used in biomedical fields [9]. Other than this, ZrO_2-scattered Ti matrix composites have been additionally expected to be high-temperature materials in the aerospace and automobile industries. ZrO_2 has unique thermal and mechanical properties, which are viable as thermal barrier functions. One of the prevalent mechanical properties of ZrO_2 is high fracture toughness because of stress-instigated change (from tetragonal to monoclinic crystal structures under pressure conditions), which can be utilized in the improvement of the fracture toughness of ceramics and ceramic matrix composites. Mechanical properties of ZrO_2 -Ti composites have been of importance in many applications industries [10]. Masatoshi Takahashi et al. [11] (2002) prepared Ti-Ag alloys 5, 10, and 20 wt% Ag) and Ti-Cu alloys (2, 5, and 10 wt% Cu) using an argon-curve dissolving heater. The composites were thrown into magnesia molds utilizing an argon gas-weight dental throwing machine, and the mechanical properties and microstructures of the castings were examined. As the centralization of silver or copper in the compounds expanded, the elasticity, yield quality, and hardness of the composites wound up higher than those of CP Ti, and the stretching of the combinations progressed toward becoming lower than that of CP Ti. Changes in the mechanical properties by alloying were viewed as brought about by strong arrangement fortifying of the α-phase and by precipitation of intermetallic compound.

The aim of the present work is to improve the Ti-based alloy for biomedical applications can be summarized as Preparation of porous CP-Ti, (Ti-Ag) and (Ti-ZrO_2) alloys with best properties by the powder metallurgy technique to use in medical applications, studying the effect of adding different weight percentages (10, 20 and 30) % of elemental Silver and Zirconia on the mechanical properties of the prepared alloys, investigated the effect of different sintering temperatures in each alloy, determining the corrosion resistance of the prepared alloys in body solution (Ringer's solution) and study some of the characteristics of specimen alloys.

2. MATERIALS AND METHODS

I. Materials

An elemental titanium powder utilized in preparing to implant alloys was from (Fluka company) and the elemental silver powder was from (Nanjing Nanotechnology) and the ceramic Zirconia powder was from (Honeywell Riedel-de Haën AG) and the properties of the powders used are shown in Table I, samples of (13mm diameter), using Powder Metallurgy technique.

Table I: Properties of (Ti, Ag, and ZrO2) powders

	Purity %	Particle size (µm)	Particle shape	Powder color	M.W
Ti	99.9	200	Spherical	Gray	47.867
Ag	99.9	149	Spherical	Gray	107.868
ZrO_2	99	45	Spherical	White	123.222

II. Methods

The starting powders were weighed (5 gm) for each sample, then blended and homogenized for (20 min.) at a speed of (42 r.p.m.) for each sample in a ball mill type (CAPCO-9VS) without balls. After Blending, the powders were cold pressed at (4 tons for 1 min.) using hydraulic Press type (MEGA-KPD-50E). Two specimens of each alloy or composite samples were prepared and sintering in two different temperatures, the sintering process of the compacted samples was carried out under high-purity argon atmosphere at (700 °C at a heating rate of 10 °C/sec for 2 hrs.) and at (900 °C at a heating rate of 10 °C/sec for 2 hrs) to get improved bonding among the green sample particles. After sintering the samples quenched in water in order to obtain hard samples, so that they bear the shocks and the surrounding conditions.

For Surface preparation, the Bakelite mounted specimens were grounded using (220, 320, 400, 600, 800, 1000, 1200, and 2000) grit emery paper of SiC to get a flat surface free from scratches and polished by using special cloth and diamond paste. Samples were then etched using a reagent that is a solution mixture of (5 ml) of nitric acid (HNO_3), (10 ml) of hydrofluoric acid (HF) and (85 ml) of water (H_2O) [12] the microscope used was of type (Model - MTM - 1A, BEL - ITALY, SN/1380).

The corrosion behavior of the samples was determined by measuring the corrosion rate of the samples in body solution (Ringer's solution) to determine the period of validity of these samples in the human body. The corrosion cell involved three electrodes connected to a potentiostat (X MTD-2MA), a saturated calomel electrode (SCE) as a reference electrode, a platinum rod as a counter electrode, and a working electrode.

The chemical composition of the testing solution is listed in Table II.

Table II: Chemical composition of Ringer's solution

Substance	Composition (g . L-1)
NaCl	8.60
KCl	0.30
CaCl2	0.33
PH	5-7.5

To find the corrosion rate using the following equation:

$$R_{mpy} = 0.13 * I_{corr.} * (e/d) \quad (1)$$

Where:

Rmpy: Corrosion penetration rate in mils per year (mpy)

Icorr: Corrosion current density ($\mu A/cm^2$)

e: Equivalent weight of the alloy

d: Alloy density ($gram^3$) [13].

The surface morphology of the samples was analyzed using SEM and EDS (Inspect TM S50-SEM), and optical microscope (Model - MTM - 1A, BEL - ITALY, SN/1380), and in order to find the composition also phase identification of each implant sample the (XRD) test was conducted by using Shimadzu (X-ray) diffractometer of type (XRD- 6000 As (3K, NOPC)).

The hardness of the samples was taken using Vickers Hardness tester of type (LARYEE Model HBRVS - 187.5). All hardness values were taken on a load of (30 kg).

3. Results and Discussion

I. SEM, EDS, and Optical Microscopic Analysis

1) For Titanium-Silver alloys

The SEM, EDS, and optical microstructure images of the (CP-Ti) and (Ti–Ag) alloys samples are shown in Figures 1-3. From the microstructure analysis, at the silver content (10 to 20 wt%) and at sintering-temperature of 700 °C and 900 °C the sample was consisted of a single phase (α-phase), with increasing the silver content to (30 wt%) an intermetallic compound (Ti_2Ag) begins to form in addition to the (α-phase)**.** It is obvious that the use of powders with differences sintering process which may affect many main properties. The addition of silver element led to the production of single-phase alloys with a high chance of producing an intermetallic compound which changes the chemical and physical properties of the alloys according to the silver content.

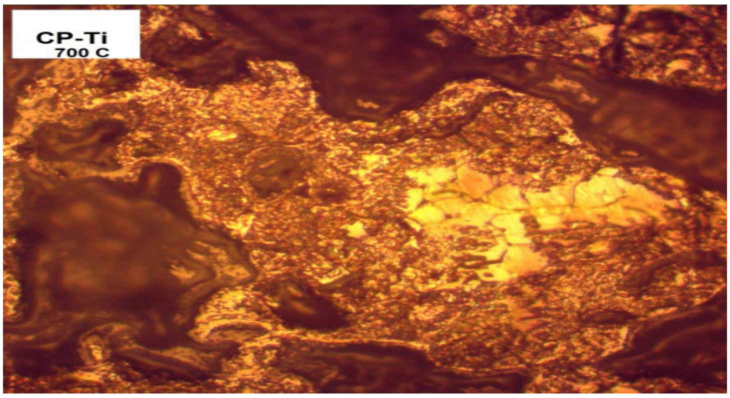

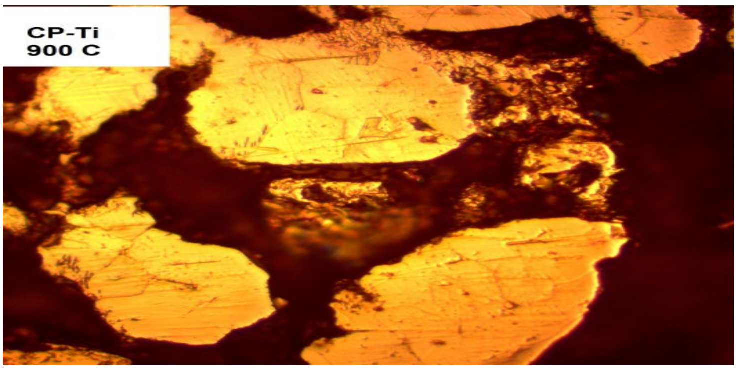

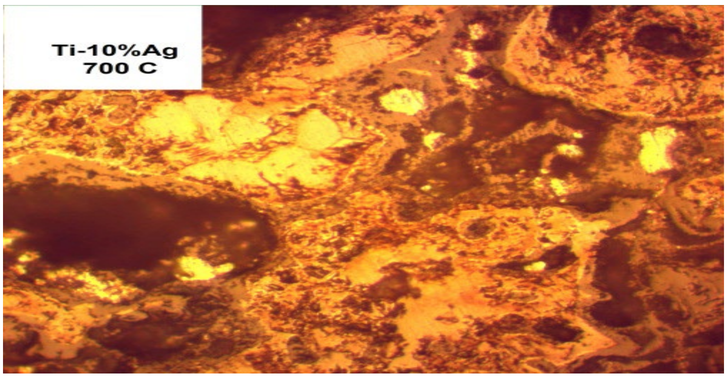

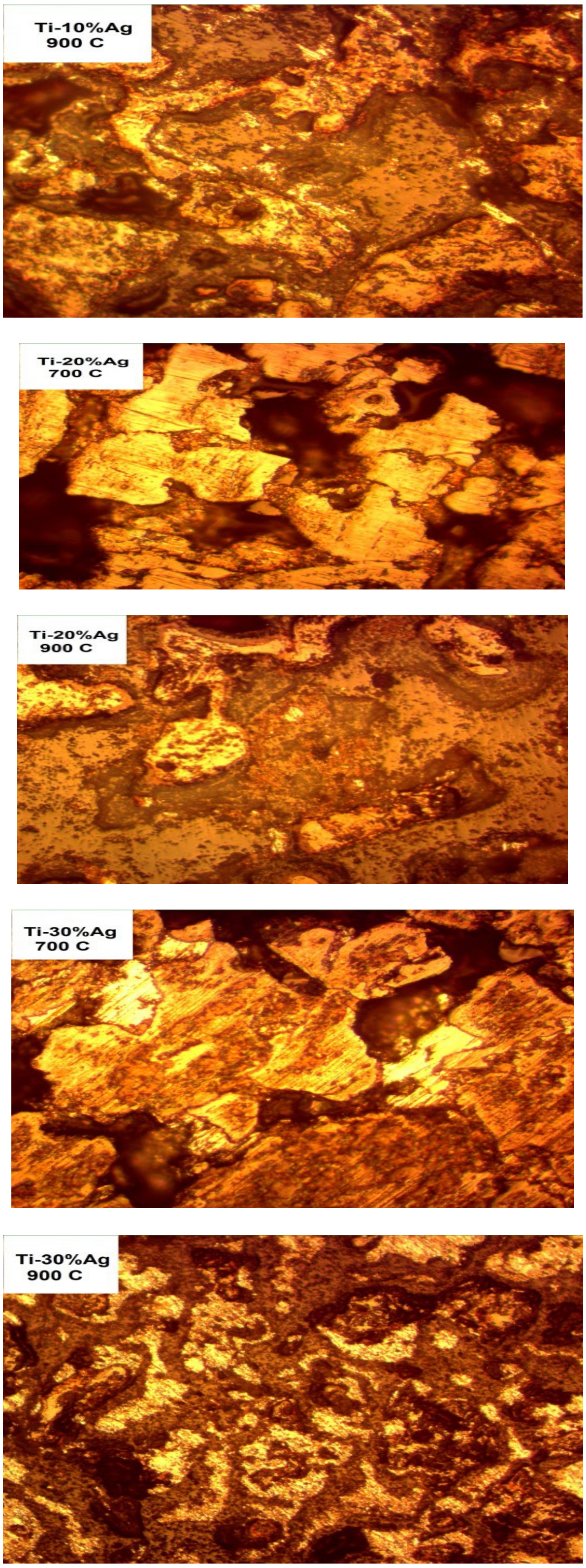

Figure 1: Optical microstructure images of the (CP-Ti) and (Ti–Ag) alloys samples at magnification force 400X.

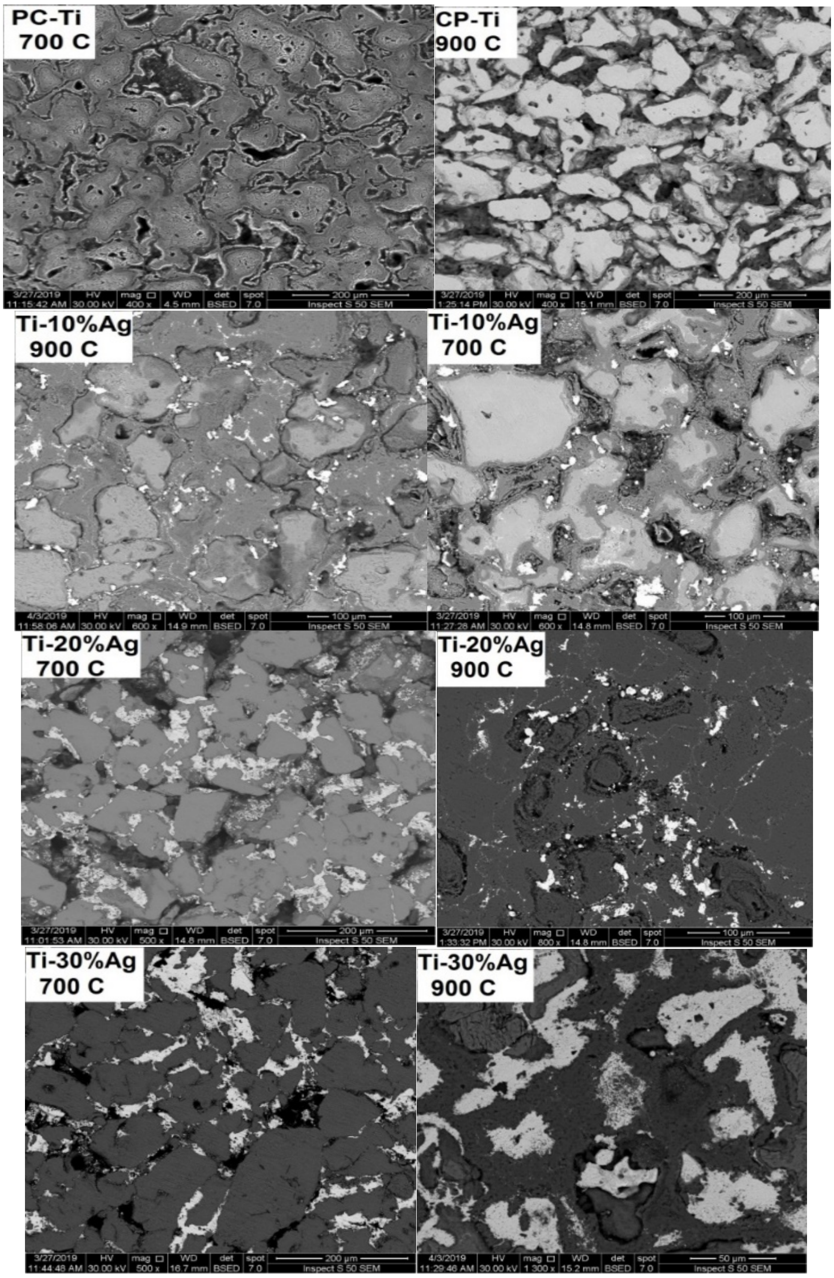

Figure 2: SEM images of the (CP-Ti) and (Ti–Ag)

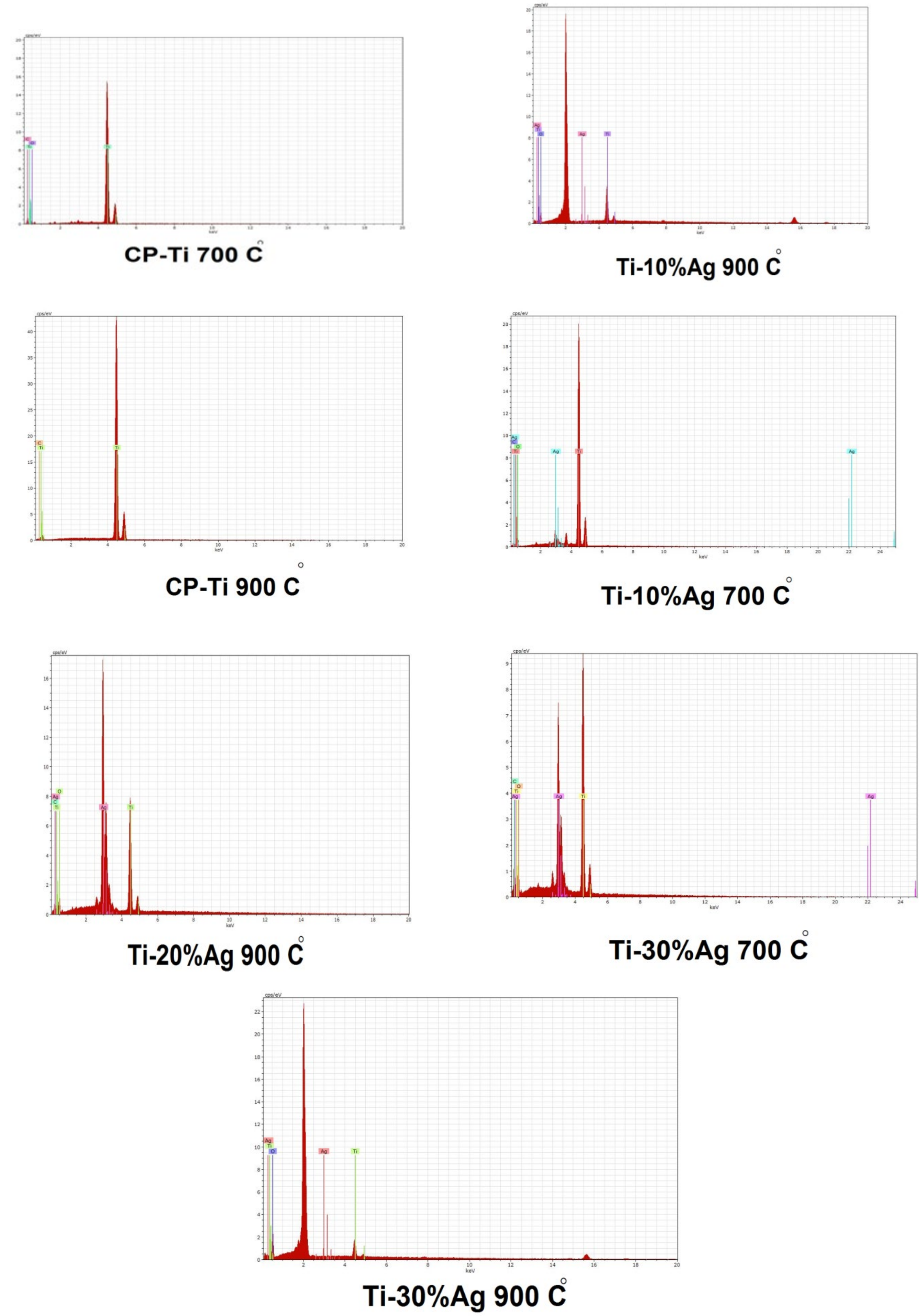

Figure 3: EDS images of pure Titanium and (Ti–Ag) alloys samples

2) For Titanium-Zirconia Composites

The SEM, EDS and optical microstructure images of the ($Ti–ZrO_2$) composite samples are shown in Figures 4-6. From the microstructure analysis, the presented phases of the alloys with Zirconia content (10 and 20 wt%) only (α-phase), with increasing the Zirconia content to (30 wt%) an intermetallic compound $(TiZr)_3O$ begins to form at the sintering temperatures of 700 °C and 900 °C**.** It is obvious that the use of powders with differences sintering process which may affect on many main properties. The addition of Zirconia ceramic led to the forming of single-phase alloys with a high chance of producing an intermetallic compound that changes the physical and chemical properties of the alloys according to the Zirconia content.

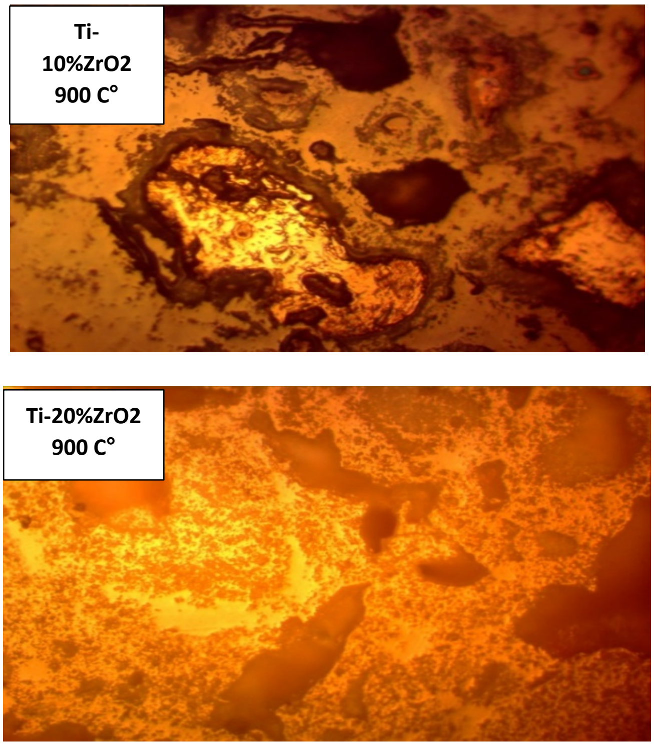

Figure 4: Optical microstructure images of (Ti–ZrO2) composite samples at magnification force 400X.

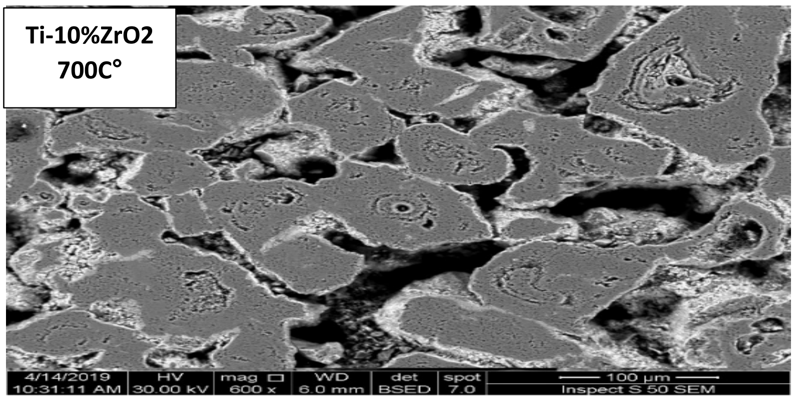

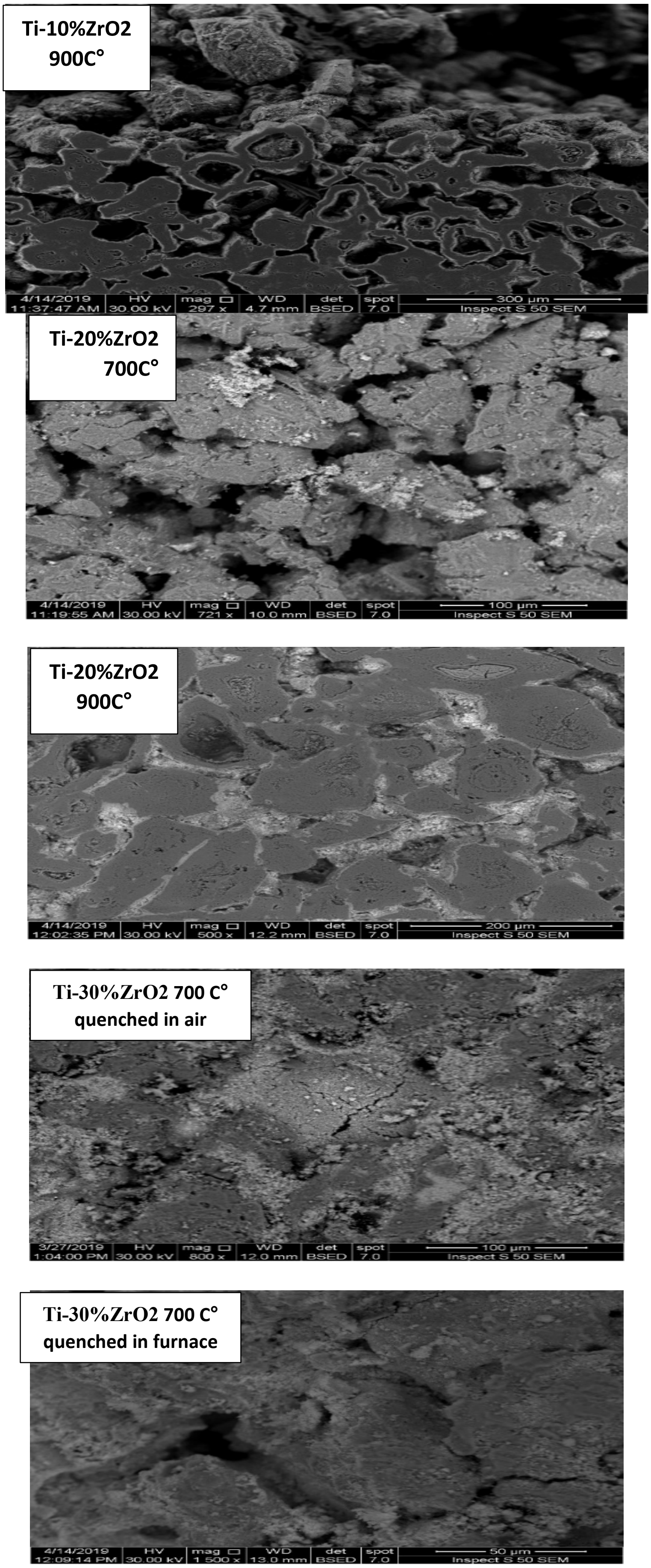
Ti-10%ZrO2
900C°
300 µm
Inspect S 50 SEM
Ti-20%ZrO2
700C°
100 µm
Inspect S 50 SEM
Ti-20%ZrO2
900C°
200 µm
Inspect S 50 SEM
Ti-30%ZrO2 700 C°
quenched in air
100 µm
Inspect S 50 SEM
Ti-30%ZrO2 700 C°
quenched in furnace
50 µm
Inspect S 50 SEM

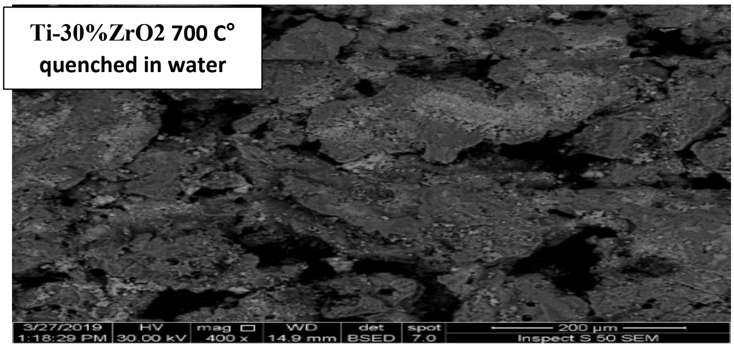

Figure 5: SEM images of the (Ti–ZrO$_2$).

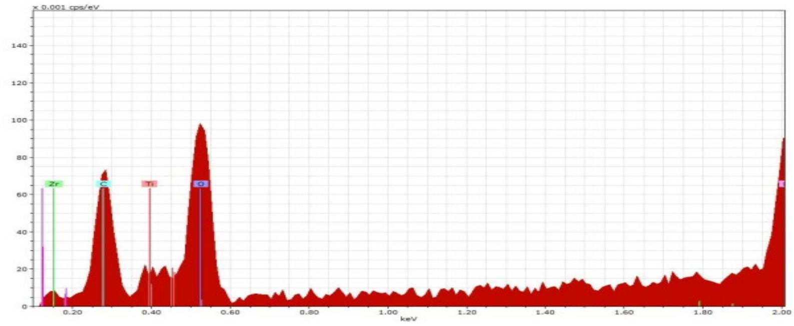

Ti-10% ZrO$_2$ 700 C°

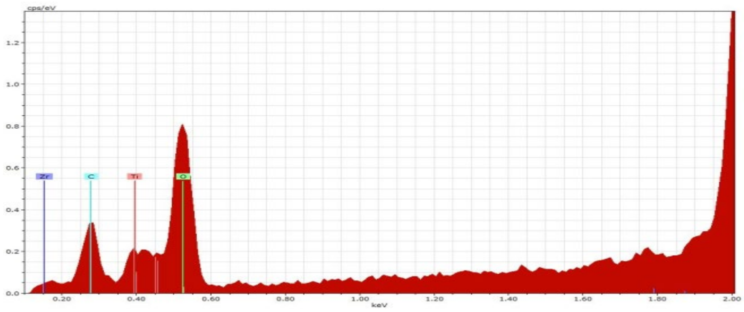

Ti-10% ZrO$_2$ 900 °C

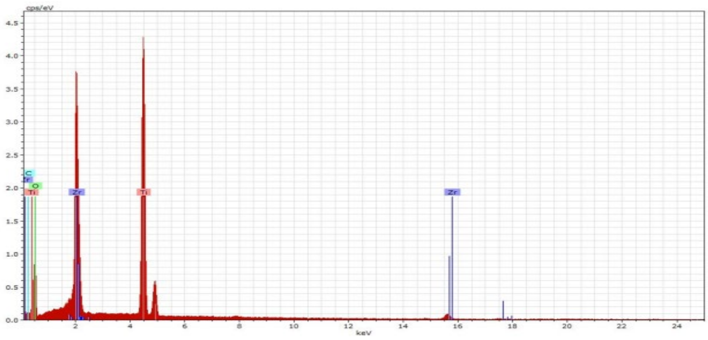

Ti-20% ZrO$_2$ 700 °C

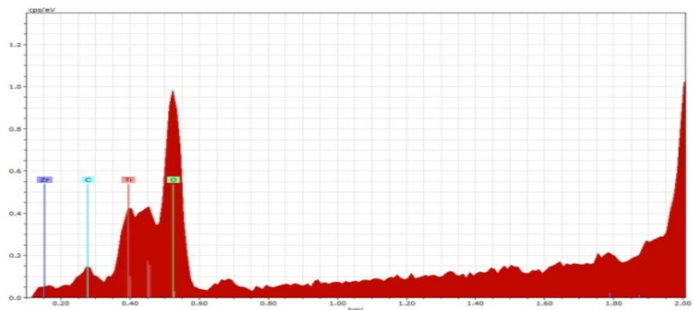

Ti-20% ZrO$_2$ 900 °C

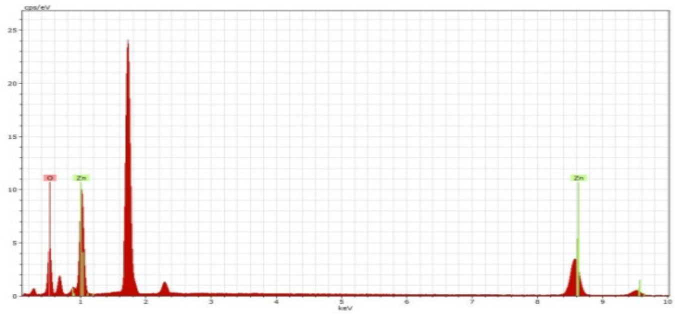

Ti-30% ZrO_2 700 °C quenched in air

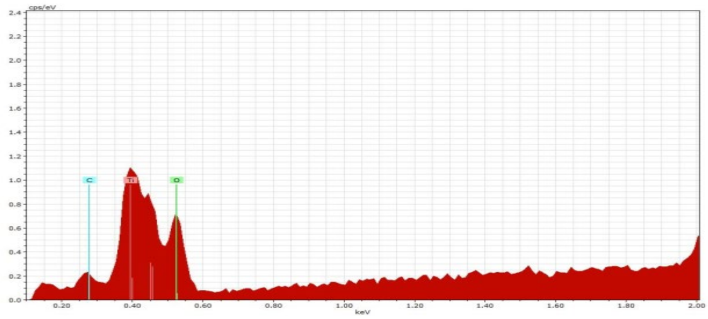

Ti-30% ZrO_2 700 °C quenched in furnace

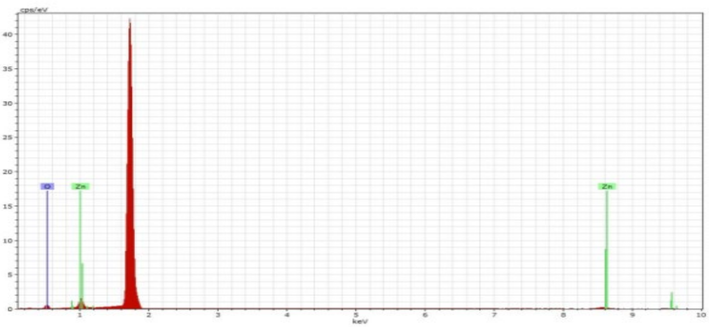

Ti-30% ZrO_2 700 °C quenched in water

Figure 6: EDS images of the (Ti–ZrO_2) alloys samples

II. X-ray Diffraction (XRD) Analysis

1) For Titanium-Silver Alloys

X-ray diffraction analysis of the CP-Ti sample revealed only the peaks of the (α-phase), as shown in Figures 7 & 8, this agrees with Mi-Kyung Han et al. [14]. The addition of Silver at (10-20 wt%) doesn't lead to the formation of a new phase or an intermetallic compound, but resulted in changing the location and intensity of the (α-phase) at sintering temperature of 900 °C and 700 °C, as shown in Figures 9-12. As the Silver content reaches (30%) an intermetallic compound is formed as shown in Figures 13 & 14 that represents the (XRD) pattern of (70%Ti-30%Ag) sample, (α-phase) was obtained along with precipitation of, (Ti_2Ag) intermetallic compound, this agrees with the previous work [15], which referred to the formation of an intermetallic compound of (Ti_2Ag).

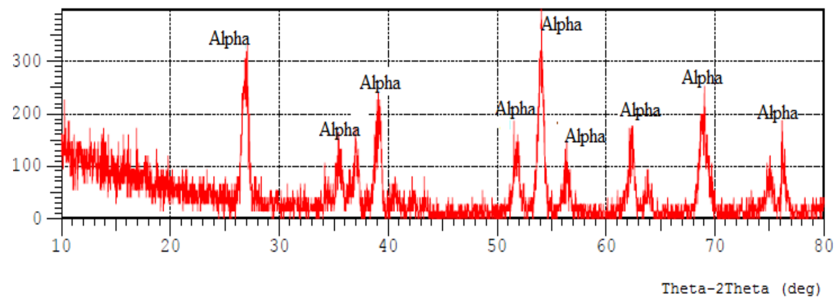

Figure 7: CP-Ti at 700 °C

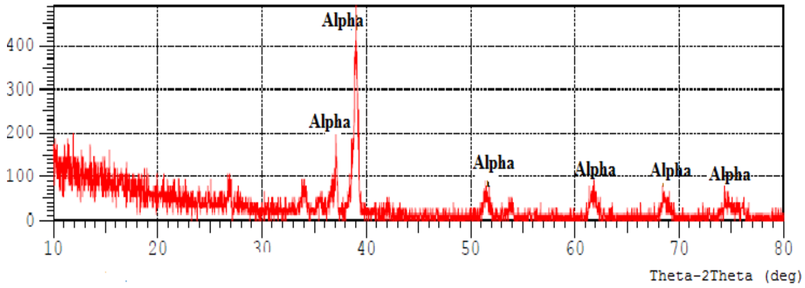

Figure 8: CP-Ti at 900 °C

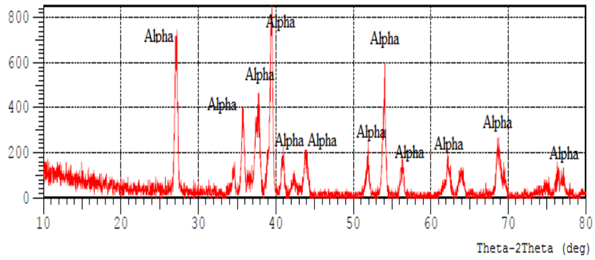

Figure 9: Ti-10%Ag at 700 °C

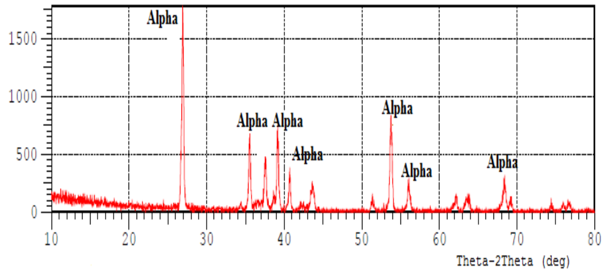

Figure 10: Ti-10%Ag at 900 °C

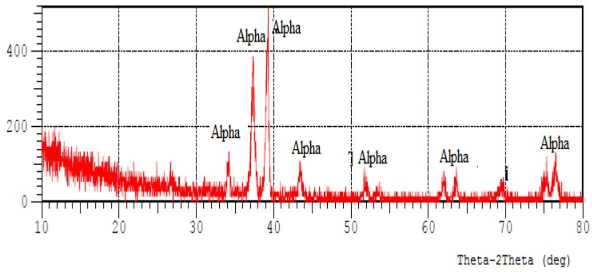

Figure 11: Ti-20%Ag at 700 °C

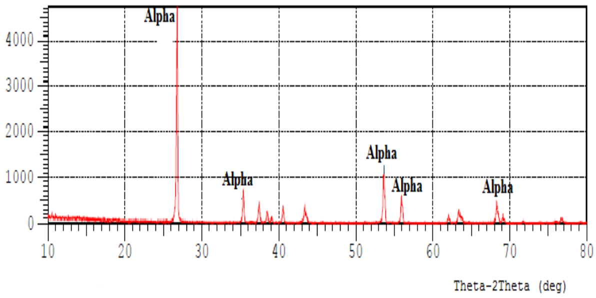

Figure 12: Ti-20%Ag at 900 °C

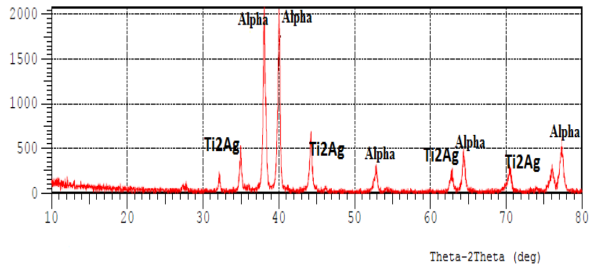

Figure 13: Ti-30%Ag at 700 °C

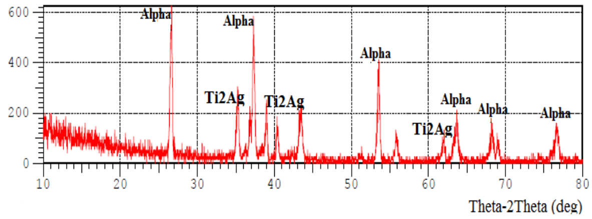

Figure 14: Ti-30%Ag at 900 °C

2) For Titanium-Zirconia Alloys

X-ray diffraction analysis shows that the addition of Zirconia at (10-20 wt%) doesn't lead to the formation of a new phase or an intermetallic compound, but resulted in changing the location and intensity of the (α-phase), as shown in Figures 15 -18. As the Zirconia content reaches (30%) an intermetallic compound $(TiZr)_3O$ was precipitated at the grain boundaries with the presence of (α-phase), as shown in Figures 19-21, All the above results agree with the ($Ti-ZrO_2$) phase diagram [16].

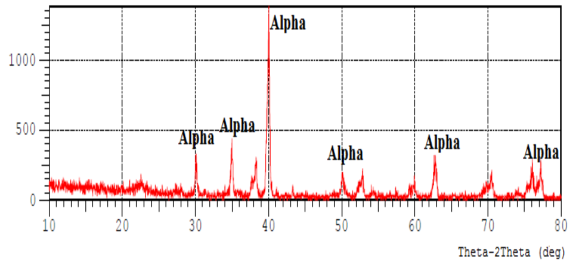

Figure 15: Ti-10% ZrO_2 at 700 °C

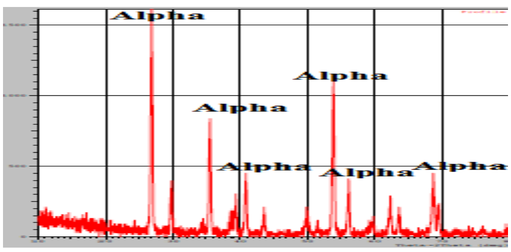

Figure 16: Ti-10% ZrO_2 at 900 °C

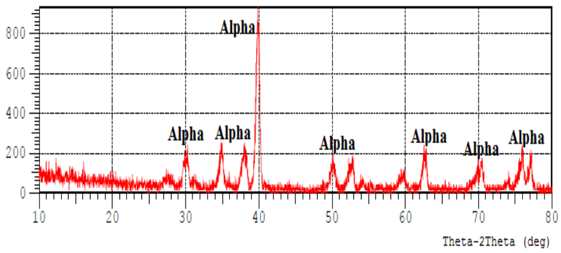

Figure 17: Ti-20% ZrO_2 at 700 °C

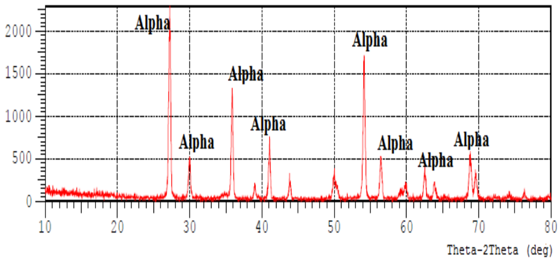

Figure 18: Ti-20% ZrO_2 at 900 °C

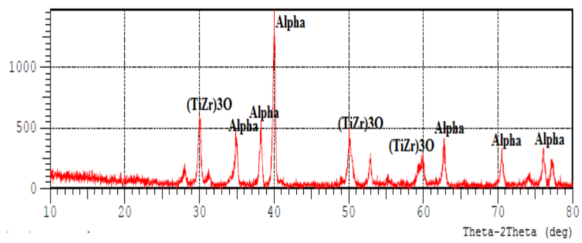

Figure 19: Ti-30% ZrO_2 at 700 °C quenched in Water

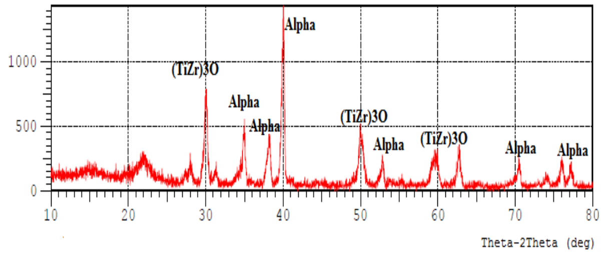

Figure 20: Ti-30% ZrO_2 at 700 °C quenched in the Air.

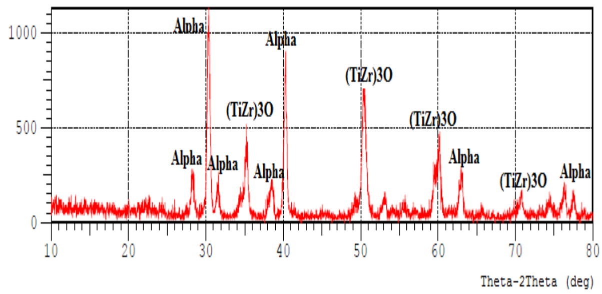

Figure 21: Ti-30%ZrO_2 at 700 °C quenched in the furnace.

III. Vickers Hardness

At a sintering temperature of 700 °C, the sample with a silver content of (90%Ti-10%Ag) presents the highest value for the hardness of (125.29 HV) while the lowest hardness value was presented by the sample of pure silver, shown Figure 22. But with the sintering temperature of 900 °C, the sample with a silver content of (70%Ti-30%Ag) had the highest value of hardness of (132.46 HV) and the lowest hardness value of (112.69HV) was with the sample of (80% Ti- 20% Ag), as shown in Figure 23. The reason for these results refers to the pore's content in the samples as the increase in pores degrade the mechanical properties due to the reduced area supporting the load. There is no significant effect of (Ti_2Ag) intermetallic compound on improving the hardness of the samples.

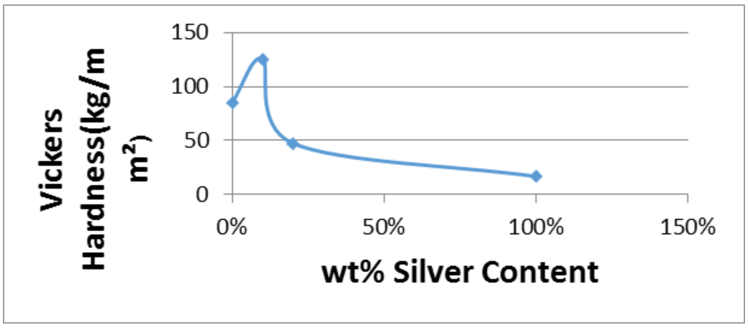

Figure 22: The Vickers hardness of the sintered samples at 700 °C at different silver contents

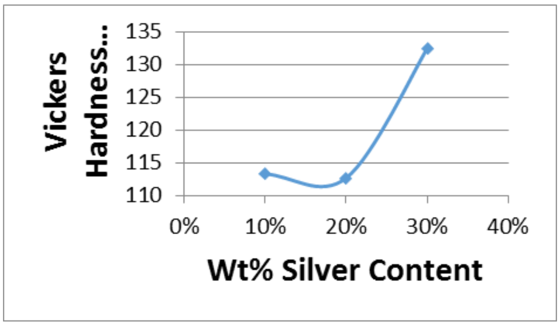

Figure 23: The Vickers hardness of the sintered samples at 900 °C at different silver contents

IV. Corrosion Behavior

1) Corrosion behavior of Titanium-Sliver alloys

At a sintering temperature of 700 °C, the results show that the corrosion resistance increases with increasing the silver content as the corrosion rate would be the best in (30% Ag) content with(0.091 mpy), as shown in Figure 24, Table III shows Corrosion Parameters of (Pure Ti) and (Titanium-Silver) samples, in Ringer's solution and in Figure 25 Tafel Curves of (Ti-Ag) alloys.

Table III: Corrosion Parameters of (Pure Ti) and (Titanium-Silver) samples, in Ringer's solution at sintering temperature of 700 °C

Composition of alloys wt%	-Ocp mV	-Ecorr. mV	icorr. μA/cm2	-bc mV/dec	+ba mV/dec	Rate of Corrosion mpy
CP-Ti	1067.3	1093.2	1.836*10-5	289.6	38.8	5.068
(90Ti-10Ag)	822.6	1054	0.4347*10-4	272	114.8	1.0729
(80Ti-20Ag)	62.5	228.6	0.15976*10-6	61.9	42.1	0.48
(70Ti-30Ag)	217.5	367.3	0.26525*10-6	60.2	147.1	0.091

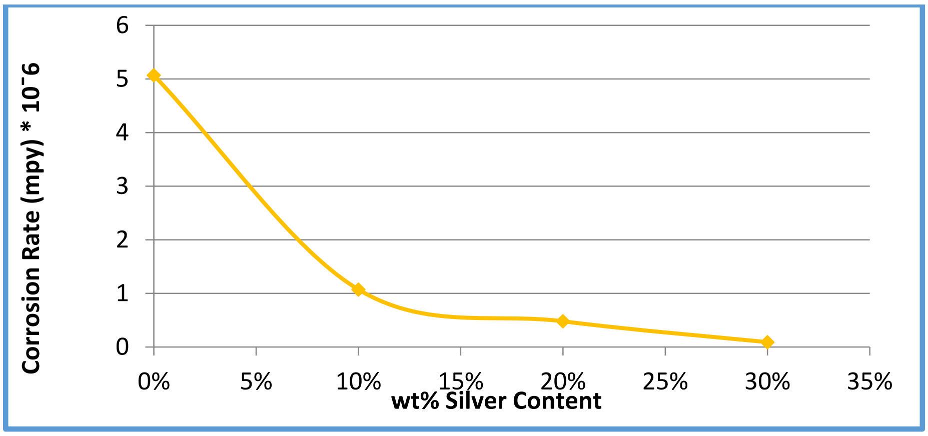

Figure 24: Corrosion rate (mpy) of (Ti-Ag) alloys at a sintering temperature of 700 °C

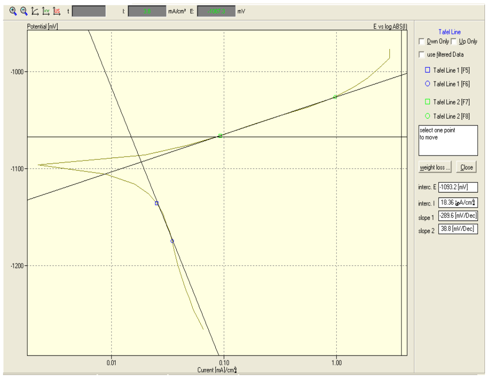

CP-Ti at 700 °C

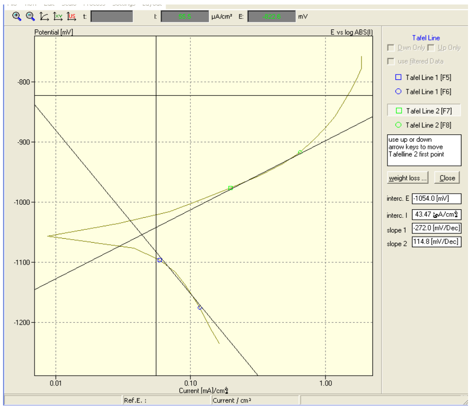

Ti-10% Ag at 700 °C

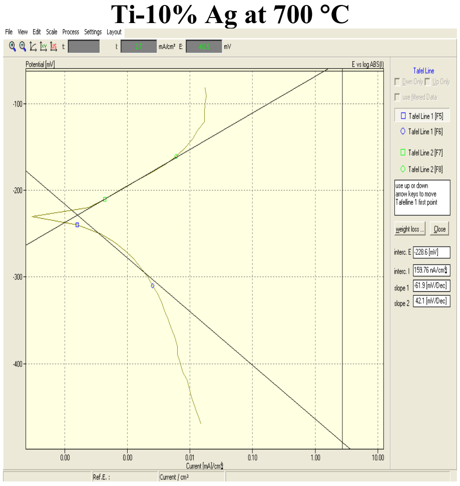

Ti-20% Ag at 700 °C

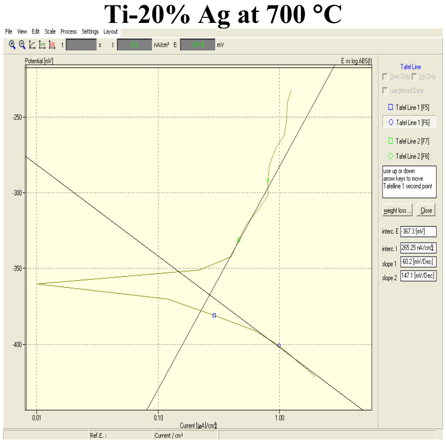

Ti-30% Ag at 700 °C

Figure 25: Tafel Curves of (Ti-Ag) alloys at the sintering temperature of 700 °C

At the sintering temperature of 900 °C, from the Figure 26 the lowest corrosion rate was with (30% Ag) and (0.059) mpy, and the highest was with CP-Ti and (10%Ag) with (5.4155) and (3.966) respectively, and that agree with the hardness results at this temperature showed in Figure 23, Table IV shows Corrosion Parameters of (CP-Ti and Ti-Ag) samples in Ringer's solution and in Figure 27: Tafel Curves of (Ti-Ag) alloys.

Table IV: Corrosion Parameters of (CP-Ti and Ti-Ag) samples in Ringer's solution at the sintering temperature of 900 °C

Composition of alloys wt%	-Ocp mV	-Ecorr. mV	icorr. μA/cm2	-bc mV/dec	+ba mV/dec	Rate of Corrosion mpy
CP-Ti	1007.2	1086.5	2.194*10-5	113.6	34.3	5.4155
(90Ti-10Ag)	1055.8	1130.9	1.454*10-5	153.3	45	3.966
(80Ti-20Ag)	1073.1	1076.7	0.3316*10-4	115.8	117.3	1.0106
(70Ti-30Ag)	297.7	376.7	0.17302*10-6	89.8	140.9	0.059

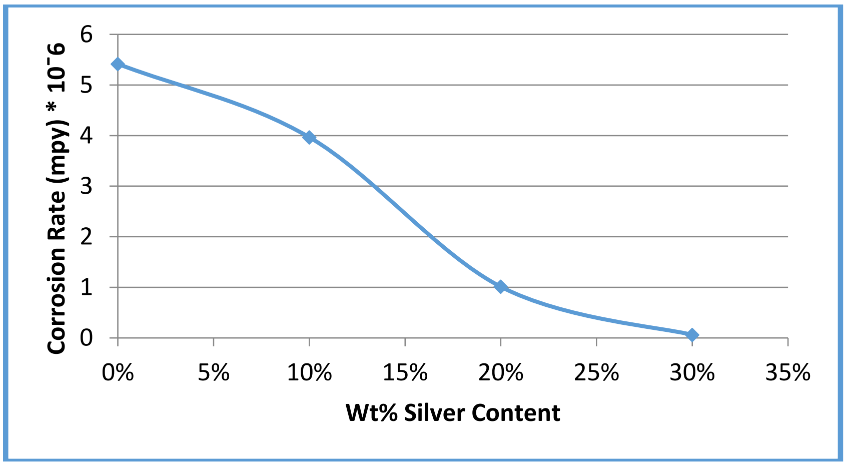

Figure 26: Corrosion rate (mpy) of (Ti-Ag) alloys at the sintering temperature of 900 °C

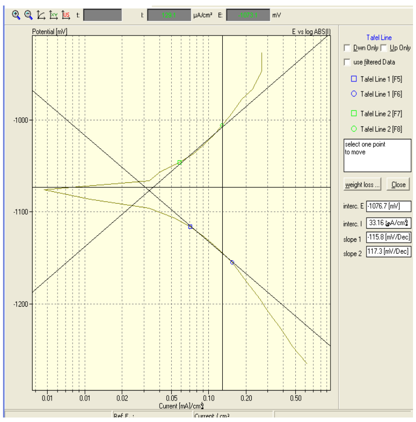

CP-Ti at 900 C°

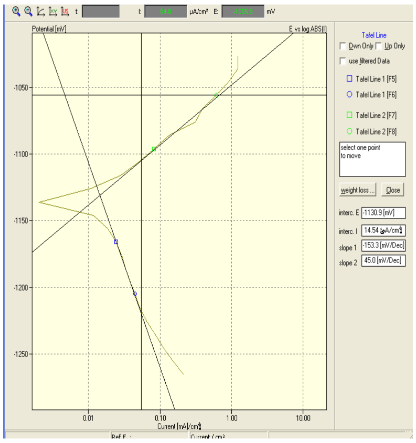

Ti-10% Ag at 900 °C

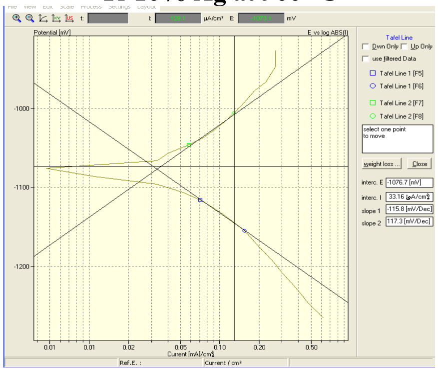

Ti-20% Ag at 900 °C

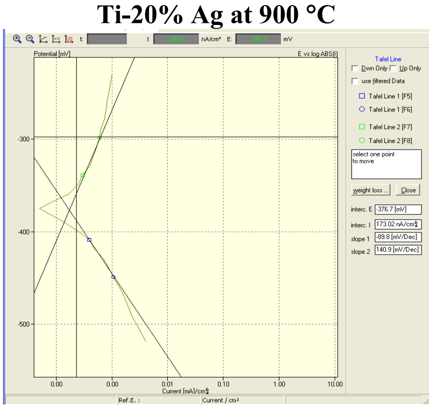

Ti-30% Ag at 900 °C

Figure 27: Tafel Curves of (Ti-Ag) alloys at the sintering temperature of 900 °C

2) Corrosion behavior for Titanium-Zirconia Alloys

The results referred to the highest corrosion rate was with (90% Ti - 10% ZrO_2) and (8.72) mpy at sintering temperature of 900 °C and the lowest value with (70%Ti-30%ZrO_2) when cooled in the air with (1.347) mpy, and thus attributed to the high percentage of porosity with increasing in Zirconia content, as shown in Figure 29, Table V shows Corrosion Parameters of (Ti-ZrO_2) samples in Ringer's solution and in Figure 28 Tafel Curves of (Ti-ZrO_2) Composites.

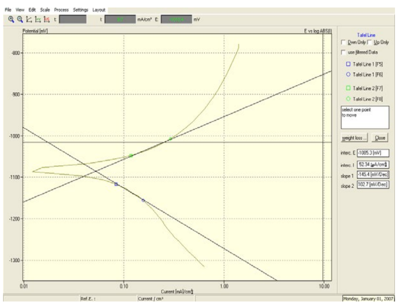

Ti-10% ZrO_2 at 700 °C

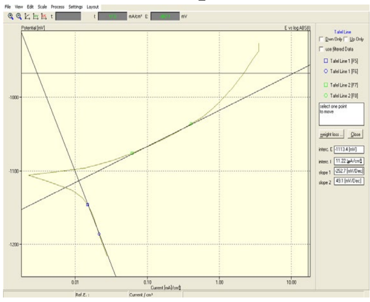

Ti-30% ZrO_2 at 700 °C quenched in the Air

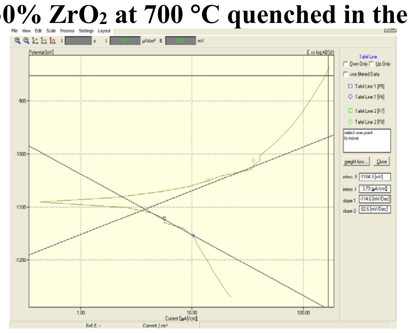

Ti-30% ZrO_2 at 700 °C quenched in the furnace

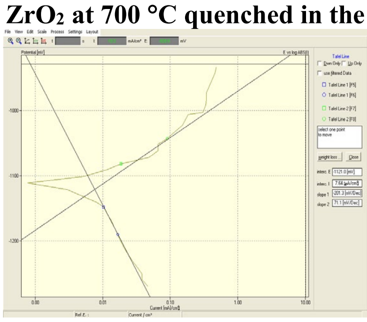

Ti-10% ZrO_2 at 900 °C

Figure 28: Tafel Curves of (Ti-ZrO_2) Composites at the sintering temperature of 700 C° and 900 °C.

Table V: Corrosion Parameters of (Ti-ZrO2) samples in Ringer's solution at sintering temperature of 700°C and 900°C

Composition of alloys wt%	-Ocp mV	-Ecorr. mV	icorr. μA/cm2	-bc mV/dec	+ba mV/dec	Rate of Corrosion mpy
(90Ti-10ZrO_2) at 700 °C	1015.4	1085.3	5.234*10-5	145.4	102.7	5.980
(70Ti-30ZrO_2) at 700 °C in Air	967.7	1113.4	1.122*10-5	252.7	49.1	1.347
(70Ti-30ZrO_2) at 700 °C in furnace	852.1	1104.3	3.79*10-6	114.6	82.6	4.55
(90Ti-10ZrO_2) at 900 °C	928.9	1121	7.64*10-6	201.3	71.1	8.72

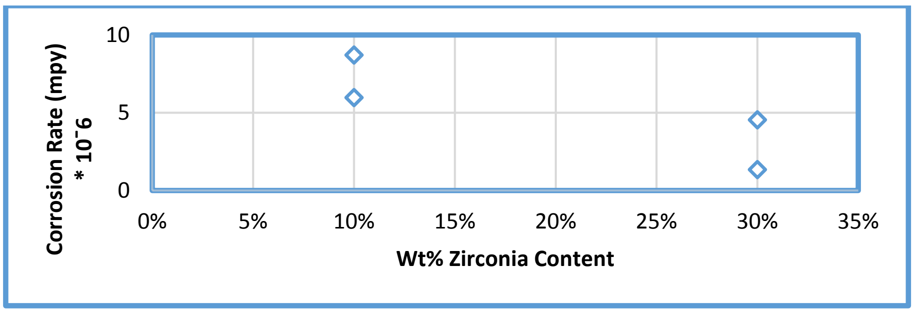

Figure 29: Corrosion rate (mpy) of (Ti-ZrO_2) composites at the sintering temperature of 700 °C and 900 °C

4. Conclusions

1- The microstructures of the samples with a silver content of (10-20 wt%) comprise of single-phase (α-phase), with increasing the silver content to (30 wt%) the alloy comprises (α-phase) and (Ti_2Ag) intermetallic compound.
2- The best hardness of titanium-silver alloys was with a silver content of (30% Wt) at the sintering temperature of 900 °C.
3- The microstructures of the samples with the Zirconia content of (10-20 wt%) comprise of single-phase (α-phase), with increasing the Zirconia content to (30 wt%) the alloy comprises (α-phase) and $(TiZr)_3O$ intermetallic compound.
4- The corrosion results showed a good corrosion resistance increases with increasing the silver content as the corrosion rate would be the best in (30% Ag) content with (0.091 mpy) at sintering temperature of 700 °C. And with a sintering temperature of 900 °C, the best result was with (30% Ag) with (0.059) mpy. In the Ti-ZrO_2 composites, the best result was with the Zirconia content of (30%ZrO_2) when cooled in the air with (1.347) mpy at sintering temperature of 700°C.

References

[1] W. Rostoker, J.O. Galante, Materials for human implantation, J. Biomech. Eng., 101 (1979)2–14. https://doi.org/10.1115/1.3426221

[2] B. D. Ratner, A. S. Hoffman, F. J. Schoen, J. E. Lemons, Biomaterials Science, San Diego: Academic Press, 37–50, 1996.

[3] M. Niinomi, Mechanical properties of biomedical titanium alloys, Mater. Sci. Eng. A, 243 (1998) 1-2, 231–236. https://doi.org/10.1016/S0921-5093(97)00806-X

[4] J. E. Davies, B. Lowenberg, A. Shiga, The bone–titanium interface in vitro, J. Biomed. Mater. Res., 24(1990) 1289-1306.https://doi.org/10.1002/jbm.820241003

[5] M. Therin, A. Meunierr, P. Christel, A histomorphometric comparison of the muscular tissue reaction to stainless steel, pure titanium and titanium alloy implant materials, J. Mater. Sci. Mater. Med., 2(1991)1–8.

[6] H. J. Breme, J. A. Helsen, Selection of materials, In: Metals as biomaterials, Scientific Research, Wiley, (1998) 1-35.

[7] B. Kasemo , Biocompatibility of titanium implants: surface science aspects, J. Prosthet. Dent., 49 (1983)832– 837. https://doi.org/10.1016/0022-3913(83)90359-1

[8] K. T. Oh, H. M. Shim, K. N. Kim, Properties of titanium-silver alloys for dental application, J. Biomed. Mater. Res. B Appl. Biomater., 74 (2005)649–658. https://doi.org/ 10.1002/jbm.b.30259

[9] A.W. Nugroho, G. Leadbeater, I.J. Davies, Processing of a porous titanium alloy from elemental powders using a solid state isothermal foaming technique, J. Mater. Sci Mater Med., 21(2010)3103-3107. https://doi.org/10.1007/s10856-010-4162-x

[10] H. Tsukamoto, Mechanical Properties of Zirconia-Titanium Composites, Int. J. Mater. Sci. Appl., 3(2014) 260-267. https://doi.org/10.11648/j.ijmsa.20140305.28

[11] M. Kikuchi, Y. Takada, Mechanical Properties and Microstructures of Dental Cast Ti-Ag and Ti-Cu Alloys, Dent. Mater. J., 21 (2002) 270-280 . https://doi.org/10.4012/dmj.21.270

[12] N. Poondla, T. Srivatsan, A. Patnaik, M. Petraroli ,A Study of the Microstructure and Hardness of two Titanium Alloys: Commercially pure and Ti–6Al–4V, J. Alloys Compd., 486 (2009) 162–167. https://doi.org/10.1016/j.jallcom.2009.06.172

[13] F. Al-Hassani, Effect of Alloying Elements on Bio-Medical Ti-Ta Shape Memory Alloys, M.Sc. Thesis, University of Technology, Iraq, 2012.

[14] M. K. Han, M. Hwang, D. Won, Y. Kim, H. Song, Y. Park, Massive Transformation in Titanium-Silver Alloys and Its Effect on Their Mechanical Properties and Corrosion Behavior, Materials, 7(2014)6194–6206. https://doi.org/10.3390/ma7096194

[15] J. L. Murray, K. J. Bhansali, The Ag-Ti (Silver-Titanium) System, Bull. Alloy Phase Diagrams, 4(1983)178–183. https://doi.org/10.1007/BF02884876

[16] R. F. Domagala, S. R. Lyon, R. Ruh, The Pseudobinary Ti-ZrO_2, J. Am. Ceram. Soc., 56 (1973)584–587.